Cellular Physiology and Biochemistry

Cell Physiol Biochem 2018;50:363-377
DOI: 10.1159/000494012
Published online: 4 October 2018
Accepted: 25 September 2018

Original Paper

Action of Protein Tyrosine Kinase Inhibitors on the Hypotonicity-Stimulated Trafficking Kinetics of Epithelial Na^+ Channels (ENaC) in Renal Epithelial Cells: Analysis Using a Mathematical Model

Rie Marunaka[a,b] Akiyuki Taruno[a] Toshiro Yamamoto[b] Narisato Kanamura[b] Yoshinori Marunaka[a,c,d,e]

[a]Department of Molecular Cell Physiology, Kyoto Prefectural University of Medicine Graduate School of Medical Science, Kyoto, [b]Department of Dental Medicine, Kyoto Prefectural University of Medicine Graduate School of Medical Science, Kyoto, [c]Japan Institute for Food Education and Health, St. Agnes' University, Kyoto, [d]Research Institute for Clinical Physiology, Kyoto Industrial Health Association, Kyoto, [e]Research Center for Drug Discovery and Pharmaceutical Development Science, Research Organization of Science and Technology, Ritsumeikan University, Kusatsu, Japan

Key Words
ENaC • Transcellular Na^+ reabsorption • Mathematical model • Simulation • Epithelium

Abstract
Background/Aims: Epithelial Na^+ channels (ENaCs) play crucial roles in control of blood pressure by determining the total amount of renal Na^+ reabsorption, which is regulated by various factors such as aldosterone, vasopressin, insulin and osmolality. The intracellular trafficking process of ENaCs regulates the amount of the ENaC-mediated Na^+ reabsorption in the collecting duct of the kidney mainly by determining the number of ENaC expressed at the apical membrane of epithelial cells. Although we previously reported protein tyrosine kinases (PTKs) contributed to the ENaC-mediated epithelial Na^+ reabsorption, we have no information on the role of PTKs in the intracellular ENaC trafficking. ***Methods:*** Using the mathematical model recently established in our laboratory, we studied the effect of PTKs inhibitors (PTKIs), AG1296 (10 μM: an inhibitor of the PDGF receptor (PDGFR)) and AG1478 (10 μM: an inhibitor of the EGF receptor (EGFR)) on the rates of the intracellular ENaC trafficking in renal epithelial A6 cells endogenously expressing ENaCs. ***Results:*** We found that application of PTKIs significantly reduced the insertion rate of ENaC to the apical membrane by 56%, the recycling rate of ENaC by 83%, the cumulative time of an individual ENaC staying in the apical membrane by 27%, the whole life-time after the first insertion of ENaC by 47%, and the cumulative Na^+ absorption by 61%, while the degradation rate was increased to 3.8-fold

R. Marunaka, A. Taruno, and Y. Marunaka contributed equally to this work.

Yoshinori Marunaka
Research Institute for Clinical Physiology, Kyoto Industrial Health Association, 67 Kitatsuboi-cho, Nishino-kyo, Nakagyo-ku, Kyoto 604-8472 (Japan)
Tel. 81-75-802-0131, E-Mail marunaka@koto.kpu-m.ac.jp

by application of PTKIs. These observations indicate that PTKs contribute to the processes of insertion, recycling and degradation of ENaC in the intracellular trafficking process under a hypotonic condition. ***Conclusion:*** The present study indicates that application of EGFR and PDGFR-inhibitable PTKIs reduced the insertion rate (k_I), and the recycling rate (k_R) of ENaCs, but increased degradation rate (k_D) in renal A6 epithelial cells under a hypotonic condition. These observations indicate that hypotonicity increases the surface expression of ENaCs by increasing the insertion rate (k_I) and the recycling rate (k_R) of ENaCs associated with a decrease in the degradation rate but without any significant effects on the endocytotic rate (k_E) in EGFR and PDGFR-related PTKs-mediated pathways.

Introduction

The transepithelial Na^+ transport mediated via epithelial Na^+ channels (ENaCs) participates in various bodily functions including regulation of the lung alveolar fluid clearance, the body fluid content, and blood pressure [1-13]. This ENaC-mediated transepithelial Na^+ transport requires the two steps across the apical and basolateral membranes of epithelial cells: 1) the first step is the entry of Na^+ across the apical membrane of epithelial cells into the intracellular space via ENaCs expressed at the apical membrane, and 2) the second step is the extrusion of Na^+ from the intracellular space across the basolateral membrane of epithelial cells mediated by the basolateral Na^+,K^+-pump located at the basolateral membrane [3, 4]. It is generally considered that the rate-limiting step in the ENaC-mediated transepithelial Na^+ transport is the Na^+ entry through the apical-membrane-located ENaC rather than the Na^+ extrusion mediated by the basolateral-membrane-located Na^+,K^+-pump. This means that the amount of ENaC-mediated transepithelial Na^+ transport is mainly regulated by the amount of the apical-membrane-located ENaC-mediated Na^+ entry, which is determined by the number of ENaCs and the activity (open probability) of individual ENaCs located at the apical membrane [3, 14-18].

Liddle's syndrome is well known as an inherited disease developing hypertension [19-22]. This syndrome is caused by over loaded body fluid volume due to a large amount of renal epithelial Na^+ reabsorption, which results from the increased number of ENaCs expressed at the apical membrane [19-22]. The wild type of ENaCs contains the binding site to Nedd4-2, an E3 ubiquitin-protein ligase degrading ENaCs [19-22]. ENaCs expressed in Liddle's syndrome are mutated with deletion or disruption of a C-terminal PY motif [19-22], increasing the number of ENaCs located at the apical membrane in Liddle's syndrome [19-22]. The number of ENaCs expressed at the apical membrane is one of the most important factors determining the amount of the ENaC-mediated transepithelial Na^+ transport (reabsorption) in the kidney, although the open probability (activity) of individual ENaC is also one of the essentially important factors determining renal Na^+ reabsorption. The insertion and endocytosis processes of ENaCs into and from the apical membrane communicating with the cytosolic ENaC store sites and the recycling and degradation processes of ENaCs determine the number of ENaCs expressed in the apical membrane. This means that the ENaC insertion into and endocytosis (retrieval) from the apical membrane and the recycling and degradation processes of ENaCs play crucial roles in determining the amount of ENaCs expressed in the apical membrane [14, 23-25].

Our previous study [26] has reported that protein tyrosine kinases (PTKs) contribute to the hypotonicity-induced up-regulation of the ENaC-mediated transepithelial Na^+ transport in renal epithelial cells. However, we still have no information on the role of PTKs in the intracellular trafficking of ENaCs in epithelial cells. We have recently established a mathematical model simulating the intracellular ENaC trafficking process [24]. Therefore, in the present study, we tried to clarify the effect of protein tyrosine kinase inhibitors (PTKIs) on the insertion, endocytotic, recycling, and degradation rates of ENaCs using an established four-state mathematical model of intracellular ENaC trafficking [24]. We here report for the first time the effects of PTKIs, AG1296 (an inhibitor of the PDGF receptor (PDGFR)) and

AG1478 (an inhibitor of the EGF receptor (EGFR)), on the intracellular ENaC trafficking process, clarifying the role of PTKs in the trafficking process.

Materials and Methods

Chemicals

NCTC-109 medium and fetal bovine serum were obtained from GIBCO (Grand Island, NY, U.S.A., and AG1296 (an inhibitor of PDGFR) and AG1478 (an inhibitor of EGFR) were purchased from Calbiochem (San Diego, CA, U.S.A.); all other chemicals from Sigma (St. Louis, MO, U.S.A.). AG1296 and AG1478 were dissolved in dimethyl sulfoxide (DMSO), the final concentration of which was 0.1%. The concentration (0.1%) of DMSO had no effect on the short-circuit current (I_{SC}).

Solutions

The hypotonic solution with the osmolality of 135 mOsm/kg H_2O contained 60 mM NaCl, 3.5 mM KCl, 1 mM $CaCl_2$, 1 mM $MgCl_2$, 10 mM HEPES, and 5 mM glucose, while the isotonic solution with the osmolality of 255 mOsm/kg H_2O contained 120 mM NaCl, 3.5 mM KCl, 1 mM $CaCl_2$, 1 mM $MgCl_2$, 10 mM HEPES, and 5 mM glucose. The pH of both solutions was adjusted to 7.4 with NaOH.

Cell culture

A6 cells, renal epithelial cells derived from the kidney of *Xenopus laevis*, were obtained from American Type Culture Collection (Rockville, MD, U.S.A.) at passage 68, and were cultured on plastic flasks in a humidified incubator in a culture medium at passages 76 ~ 84. The composition of the culture media was 75% (v/v) NCTC-109 (Sigma-Aldrich, Inc.), 15% (v/v) distilled water and 10% (v/v) fetal bovine serum at 27°C and 1.0% CO_2 in air [27]. We measured I_{SC} from A6 cells seeded at a density of 5 x 10^4 A6 cells/well onto tissue culture-treated Transwell filter cups (polycarbonate porous membranes; Costar Corporation, Cambridge, MA, USA) and cultured for 13 - 15 days. The A6 cells of approximately 3 x 10^6 cells/Transwell filter cup cultured for 13 - 15 days formed a monolayer.

Measurements of short-circuit current (I_{SC}) under a hypotonic condition and application of PTKIs, AG1296 (10 μM: an inhibitor of PDGFR) and AG1478 (10 μM: an inhibitor of EGFR)

We measured I_{SC} from cultured A6 cells monolayer on the Transwell filter cup transferred to a modified Ussing chamber (Jim's Instrument, Iowa City, IA, U.S.A.) designed to hold the Transwell filter cup by clamping the transepithelial electrical-potential-difference to 0 mV using a high-impedance millivoltmeter (VCC-600, Physiologic Instrument, San Diego, CA, U.S.A.) [24, 28, 29] in the hypotonic solution with and without PTKIs, AG1296 (10 μM) and AG1478 (10 μM). In the present study, a positive current means a net flow of cations from the apical to the basolateral solutions; i.e., the transepithelial Na^+ absorption is represented as a positive current (I_{SC}). The bathing solution was stirred by bubbling with 21 % O_2 / 79 % N_2. During the I_{SC} measuring time period, 24 h, no amino acids or serum was supplied to the bathing hypotonic solution.

The benzamil-sensitive I_{SC}

The hypotonicity-induced Isc was almost completely blocked by 10 μM benzamil, a specific blocker of ENaCs [30] added to the apical solution 24 h after application of the hypotonicity, as previously shown [23, 31]. Further, in the apical solution containing 10 μM benzamil, the application of hypotonicity did not induce any significant I_{SC}. Therefore, the hypotonicity-induced I_{SC} consists of the ENaC-mediated current.

Temperature

Since A6 cells are derived from the kidney of *Xenopus laevis* (an amphibian cell line), all experiments were performed at 22 ~ 23°C.

Data presentation and statistics

Results shown in Tables are expressed as the mean ± standard error (S.E.). Statistical significance was determined by Student's *t*-test, and $p < 0.05$ was considered significant.

Results

Simulation of intracellular ENaC trafficking

Our previous study [24] has established a four-state mathematical model of ENaC trafficking (Fig. 1) with the following components: an insertion state (Insert) of ENaCs that can be trafficked to the apical membrane with the insertion rate, k_I; an apical membrane state (Apical) where Na^+-conducting ENaCs stay; a recycling state (Recycl) where ENaCs are retrieved from an apical membrane state (Apical) with the endocytotic rate, k_E, and then trafficked to the insert state (Insert) with the recycling rate, k_R, communicating with the apical membrane state (Apical), or to a degradation state (Degrad) with the degradation rate, k_D (see Fig. 1). As reported in our previous study [24], the change in the amount of ENaCs staying at each state is represented by the following differential equation (see equation (1) - (4)).

$$\frac{d\,Insert(t)}{dt} = -k_I\,Insert(t) + k_R\,Recycl(t) \quad (1),$$

$$\frac{d\,Apical(t)}{dt} = k_I\,Insert(t) - k_E\,Apical(t) \quad (2),$$

$$\frac{d\,Recycl(t)}{dt} = k_E\,Apical(t) - (k_R + k_D)\,Recyc(t) \quad (3),$$

$$\frac{d\,Degrad(t)}{dt} = k_D\,Recycl(t) \quad (4),$$

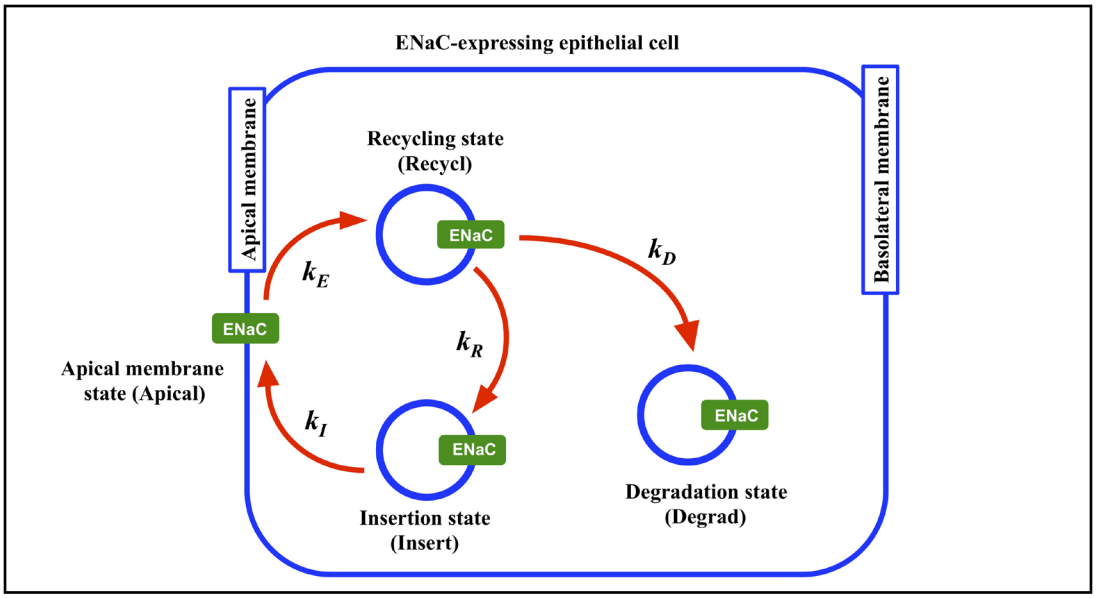

Fig. 1. An intracellular ENaC trafficking model. 1) An insertion state (Insert): this state contains ENaCs that access to the apical membrane with an insertion rate into the apical membrane (k_I). 2) An apical membrane state (Apical): this state contains ENaCs that function as Na^+-conducting (permeant) pathways across the apical membrane. 3) An recycling state (Recycl): this state contains ENaCs retrieved from the apical membrane with an endocytotic rate (k_E), and then the ENaCs are back to the insertion state (Insert) with a recycling rate (k_R), or to a degradation pathway (Degrad) with a degradation rate (k_D). *Insert (t)* is the amount of ENaCs localized at the insertion state, Insert, at time = *t*. *Apical (t)* is the amount of ENaCs localized at the apical membrane state, Apical, at time = *t*. *Recycle (t)* is the amount of ENaCs localized at the recycling state, Recycl, at time = *t*. *Degrad (t)* is the amount of ENaCs localized at the degradation state, Degrad, at time = *t*. *t* is the time elapsed after applying the hypotonic condition to the cells.

where t is the time elapsed after application of a hypotonic solution with or without 10 μM AG1296 and 10 μM AG1478, and *Insert* (t), *Apical* (t), *Recycl* (t) and *Degrad* (t) are respectively the amounts of ENaCs staying at the insertion state (Insert), the apical membrane state (Apical), the recycling state (Recycl) and the degradation state (Degrad) at time = t. We defined respectively $Insert_0$, $Apical_0$, $Recycl_0$ and $Degrad_0$ as the values of the variables, *Insert*, *Apical*, *Recycl* and *Degrad* just before application of hypotonicity (i.e., the values of *Insert*, *Apical*, *Recycl* and *Degrad* at time (t) = zero), a general solution for each variable can be obtained as follows:

$$Insert\,(t) = C_1\frac{k_E + l}{k_I}exp(lt) + C_2\frac{k_E + m}{k_I}exp(mt) + C_3\frac{k_E + n}{k_I}exp(nt) \quad (5),$$

$$Apical\,(t) = C_1\,exp(lt) + C_2\,exp(mt) + C_3\,exp(nt) \quad (6),$$

$$Recycl\,(t) = C_1\frac{(k_I + l)(k_E + l)}{k_I\,k_R}exp(lt) + C_2\frac{(k_I + m)(k_E + m)}{k_I\,k_R}exp(mt) + C_3\frac{(k_I + n)(k_E + n)}{k_I\,k_R}exp(nt) \quad (7),$$

$$Degrad\,(t) = C_1\frac{k_D(k_I + l)(k_E + l)}{k_I\,k_R\,l}exp(lt) + C_2\frac{k_D(k_I + m)(k_E + m)}{k_I\,k_R\,m}exp(mt) + C_3\frac{k_D(k_I + n)(k_E + n)}{k_I\,k_R\,n}exp(nt) + C_4 \quad (8).$$

The following equations (9), (10), (11) and (12) respectively provide C_1, C_2, C_3 and C_4 appearing in equations (5), (6), (7) and (8), while l, m or n is one of the three roots, r, of the cubic equation (13) (c.f., Cardano's Formula for cubic equation):

$$C_1 = \frac{k_I(k_I + k_E + m + n)\,Insert_0 - (k_E + m)(k_E + n)\,Apical_0 - k_I k_R\,Recycl_0}{(l - m)(n - l)} \quad (9),$$

$$C_2 = \frac{k_I(k_I + k_E + l + n)\,Inseet_0 - (k_E + l)(k_E + n)\,Apical_0 - k_I k_R\,Recycl_0}{(l - m)(m - n)} \quad (10),$$

$$C_3 = \frac{k_I(k_I + k_E + l + m)\,Insert_0 - (k_E + l)(k_E + m)\,Apical_0 - k_I k_R\,Recycl_0}{(m - n)(n - l)} \quad (11),$$

$$C_4 = Degrad_0 + \frac{k_D}{k_R\,l\,m\,n}\{[k_I k_E(k_I + k_E + l + m + n) - lmn]\,Insert_0 - (k_E + l)(k_E + m)(k_E + n)\,Apical_0 - k_I k_E k_R\,Recycl_0\} \quad (12),$$

$$r^3 + (k_I + k_E + k_R + k_D)r^2 + (k_I k_E + k_I k_R + k_I k_D + k_E k_R + k_E k_D)r + k_I k_E k_D = 0 \quad (13).$$

The most parts of the hypotonicity-stimulated I_{SC} were blocked I_{SC} by benzamil, a specific inhibitor of ENaC [32], added after the application of hypotonicity [23, 26, 31, 33-35], and the application of 10 μM benzamil to the apical solution almost completely diminished the hypotonicity-induced I_{SC}. Therefore, the hypotonicity-induced I_{SC} consists of

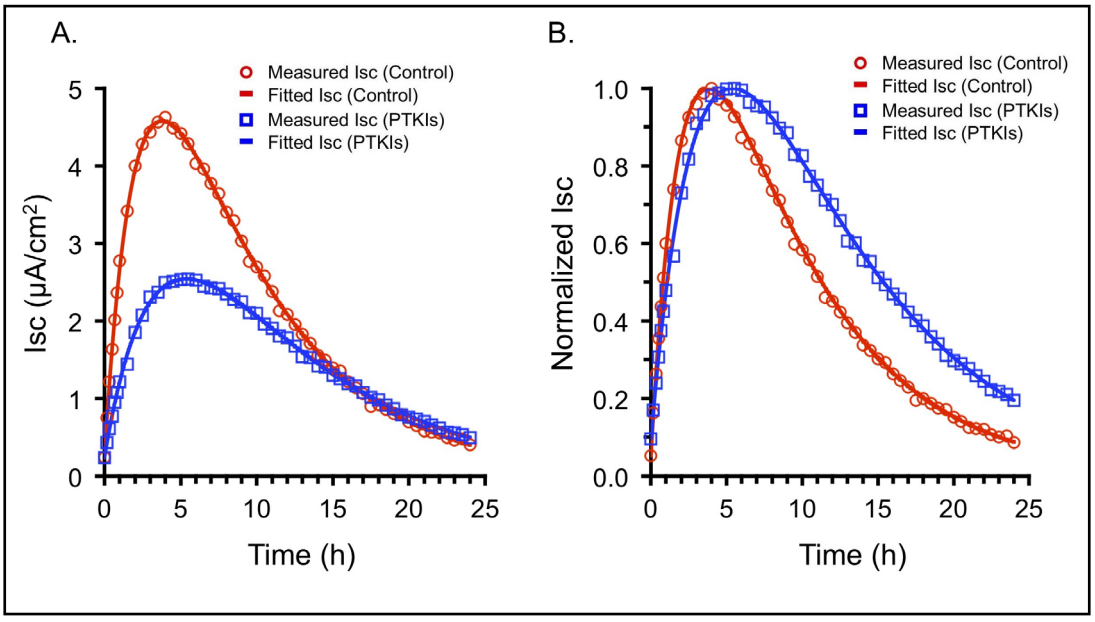

Fig. 2. Hypotonicity-induced short-circuit currents (I_{SC}) and fitted (simulated) I_{SC} obtained using a four-state mathematical model. A) Red circles and line respectively indicate a typical control time course of experimentally observed hypotonicity-induced I_{SC} (red circles) and the fitted (simulated) I_{SC} using equation (6) (red line) in the absence of PTKIs (control). Blue squares and line respectively indicate a typical time course of hypotonicity-induced I_{SC} (blue squares) and our model's prediction of I_{SC} (blue line) in the presence of PTKIs, AG1296 (10 μM) and AG1478 (10 μM). B) Normalized Isc to each peak value of Isc = 1. Red circles and line respectively show the normalized Isc in the absence of PTKIs (control). Blue squares and line respectively show the normalized Isc in the presence of PTKIs (control).

the ENaC-mediated current indicating that the hypotonicity-induced I_{SC} is generated by the ENaC-mediated transepithelial Na^+ transport. We have also reported that the application of hypotonicity elevates the ENaC-mediated I_{SC} by increasing the number of ENaCs staying in the apical membrane but not the activity (open probability) of individual ENaCs [34]. This means that hypotonicity increases the number of ENaC staying at the apical membrane by regulating the intracellular ENaC trafficking without any effects on ENaC activity. Hypotonicity induced a biphasic change in I_{SC}: an increase followed by a decrease in I_{SC} without application of PTKIs (control) (red circles in Fig. 2A). Although hypotonic stress also showed a biphasic change in I_{SC} even in the presence of PTKIs, AG1296 (10 μM) and AG1478 (10 μM) (blue squares in Fig. 2A) similar to control (without of PTKI), application of PTKIs decreased the hypotonicity-induced I_{SC} (Fig. 2A). *Apical* (t) is the amount of ENaCs staying at the apical membrane state (Apical in Fig. 1) at time = t. This means that I_{SC} (t) is proportional to *Apical* (t), where I_{SC} (t) is I_{SC} at time = t under conditions that ENaCs have constant activity (open probability). Based on the facts, we fitted the value of *Apical* (t) represented by equation (6) to the experimentally observed I_{SC} (red circles without application of PTKIs (control) and blue squares with application of PTKIs (PTKI) in Fig. 2A) using equations (9) - (13), and we obtained the values of k_I, k_E, k_R and k_D. Solid lines in Fig. 2A show the simulated I_{SC} obtained from the fitting of equation (6) to the experimentally measured I_{SC}: the red solid line shows the fitted I_{SC} without application of PTKIs (control: Fig. 2A), and the blue solid line shows the fitted I_{SC} in the presence of PTKI, AG1296 (10 μM) and AG1478 (10 μM) (Fig. 2A). Fig. 2B shows the experimentally observed I_{SC} and the simulated I_{SC} in the absence or presence of PTKIs normalized to each peak value of I_{SC} under each condition, respectively. Interesting, I_{SC} in without PTKIs (control in Fig. 2B) reached a peak at an earlier time and faster decreased than that in the presence of PTKIs (PTKI in Fig. 2B). As mentioned above, we obtained the values of k_I, k_E, k_R and k_D via the fitting process, which are shown in Table 1. Application of AG1296 (10 μM) and AG1478 (10 μM)

significantly reduced k_I of ENaC to the apical membrane by 56%, and k_R of ENaC by 83%, but increased k_D to 3.8-fold without any significant effect on k_E.

Table 1. Evaluated values of ENaC's trafficking rates in the absence (control) and presence of PTKIs, AG1296 (10 μM) and AG1478 (10 μM). *, significantly different between control (n = 6) and PTKIs (n = 6) at $p < 0.005$. #, significantly different between control (n = 6) and PTKIs (n = 6) at $p < 0.01$. ##, significantly different between control (n = 6) and PTKIs (n = 6) at $p < 0.001$. NS, no significant difference between control (n = 6) and PTKIs (n = 6)

Condition	Insertion k_I (h^{-1})	Endocytosis k_E (h^{-1})	Recycling k_R (h^{-1})	Degradation k_D (h^{-1})
Control	0.414 ± 0.050	0.251 ± 0.008	0.357 ± 0.092	0.896 ± 0.135
PTKIs	0.183 ± 0.024 *	0.272 ± 0.041 NS	0.059 ± 0.008 #	3.363 ± 0.487 ##

Fig. 3A shows the amount of ENaCs localized at each state shown in Fig. 1: *Insert* (*t*) is the amount of ENaC localized at the insertion state (Insert), at time = *t*; *Apical* (*t*) is the amount of ENaCs localized at the apical membrane state (Apical), at time = *t*; *Recycl* (*t*) s the amount of ENaCs localized at the recycling state (Recycl), at time = *t*; *Degrad* (*t*) is the amount of ENaCs localized at the degradation state (Degrad), at time = *t*, where *t* is the time elapsed after application of a hypotonic solution to the cells. The solid and dotted lines respectively show the amounts in the absence (control) and presence of PTKIs. Panels a, b c, and d in Fig. 3B represent respectively the amounts of ENaCs localized at *Insert* (*t*), *Apical* (*t*), *Recycl* (*t*) and *Degrad* (*t*). The amount of ENaC localized at the insertion state (Insert), *Insert* (*t*), decreased faster in the absence of PTKIs (control: the red solid line in Fig. 3B-a) than that in the present of PTKIs (the blue dotted line in Fig. 3B-a). This phenomenon would occur mainly due to the larger value of k_I in the absence of PTKIs (control) than that in the presence of PTKIs (Table 1). The amount of ENaC localized at the apical membrane state (Apical), *Apical* (*t*), faster increased followed by faster diminution in the absence of PTKIs (control: the red solid line in Fig. 3B-b) compared with that in the presence of PTKIs (the blue dotted line in Fig. 3B-b). The phenomenon observed in the rising phase of *Apical* (*t*) would be mainly due to the larger value of k_I in the absence of PTKIs (control) than that in the presence of PTKIs (Table 1). The falling phase of *Apical* (*t*) with a faster rate observed in the absence of PTKIs (control) shown in Fig. 3B-b would be caused by faster depletion of the ENaC amount at the insertion state (Insert) (the ENaC source to the apical state) in the absence of PTKIs (control in Fig. 3B-a) compared with that in the presence of PTKIs (PTKI in Fig. 3B-a). The amount of ENaCs localized at the recycling state (Recycl), *Recycl* (*t*), was much larger in the absence of PTKIs (control: the red solid line in Fig. 3B-c) than that in the presence of PTKIs (the blue dotted line in Fig. 3B-c). This phenomenon would be due to the larger amount of ENaC localized at the apical membrane (Apical), *Apical* (*t*), in the absence of PTKIs (control) than that in the presence of PTKIs (Fig. 3B-b) and the larger value of k_R and smaller value of k_E in the absence of PTKIs than that in the presence of PTKIs (Table 1). The amount of ENaC localized at the degradation state (Degrad), *Degrad* (*t*), a little bit faster increased in the absence of PTKIs (control: the red solid line in Fig. 3B-d) than that in the presence of PTKIs (the blue dotted line in Fig. 3B-d). This phenomenon would be caused by the larger amount of ENaC at the recycling state (Recycl), *Degrad* (*t*), in the absence of PTKIs (control) than that in the presence of PTKIs (Fig. 3B-c) even though the value of k_D in the absence of PTKIs (control) was much smaller than that in the presence of PTKIs (Table 1).

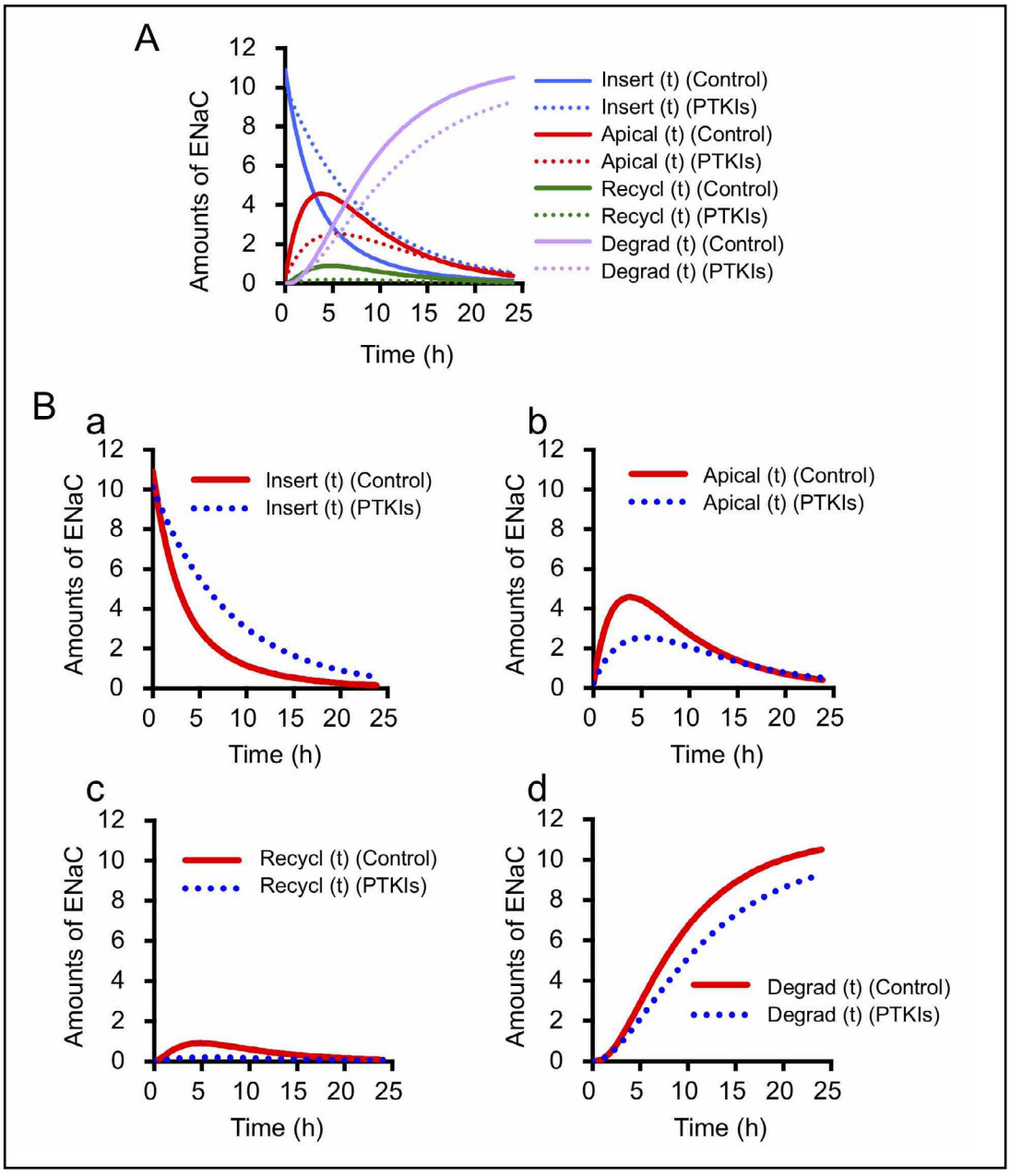

Fig. 3. Time-dependent changes in the amounts of ENaCs localized at four states, Insert, Apical, Recycl and Degrad, shown in Fig. 1. A) Solid and dotted lines respectively indicate the amounts of ENaCs localized at each four-state in the absence (control) and presence of PTKIs, AG1296 (10 μM) and AG1478 (10 μM). Four states consist of an insertion state (Insert: blue lines), an apical membrane state (Apical: red lines), a recycling state (Recycl: green lines), and a degradation state (Degrad: purple lines) as shown in Fig. 1. *Insert (t)* (blue lines) shows the amount of ENaC localized at a state, Insert, at time = *t*: *Apical (t)* (red lines), the amount of ENaCs localized at a state, Apical, at time = *t*: *Recycl (t)* (green lines), the amount of ENaCs localized at a state, Recycl, at time = *t*: *Degrad (t)* (purple lines), the amount of ENaCs localized at a state, Degrad, at time = *t*. *t* is the time elapsed after exposure of the cells to the hypotonic solution. *Insert (t)*, *Apical (t)*, *Recycl (t)* and *Degrad (t)* respectively represented by equations (5), (6), (7) and (8) are described using the values of k_I, k_E, k_R and k_D determined by fitting *Apical (t)* to the experimentally observed I_{SC}. B) The panels, a, b, c, and d respectively show *Insert (t)*, *Apical (t)*, *Recycl (t)* and *Degrad (t)* in the absence (control: red solid lines) and presence (blue dotted lines) of PTKIs, AG1296 (10 μM) and AG1478 (10 μM).

Recycling ratio of endocytotic ENaCs to the apical membrane; R_R

The endocytotic ENaCs move into the recycling state (Recycl). These ENaCs located at the recycling state (Recycl) have two opportunities as moving sites: 1) the insertion state (Insert) (Fig. 1) or 2) the degradation state (Degrad) (Fig. 1). The recycling ratio of ENaC (R_R) is represented by the following equation.

$$R_R = \frac{k_R[\mathrm{ENaC}]_{\mathrm{Recycl}}}{k_R[\mathrm{ENaC}]_{\mathrm{Recycl}} + k_D[\mathrm{ENaC}]_{\mathrm{Recycl}}} = \frac{k_R}{k_R + k_D} \qquad (14),$$

where $[\mathrm{ENaC}]_{\mathrm{Recycl}}$ is the amount of ENaCs staying at the recycling state (Recycl). As shown in Table 2, retrieved ENaCs of 28% would be recycled to the insertion state (Insert) under control conditions of hypotonic stress without PTKIs, and PTKIs almost completely blocked the recycle of ENaCs to the insertion state (Insert in Fig. 1) from the recycling state (Recycl in Fig. 1) (R_R = 2% in the presence of PTKIs, meaning most of endocytic ENaCs are degraded without recycling). This means that PTKs facilitate the transition of ENaCs from the recycling state (Recycl in Fig. 1) back to the insertion state (Insert in Fig. 1) with the ENaC's recycling ratio, $R_R = (k_R/(k_R + k_D))$ (Table 2), by both increasing the recycling rate (k_R) and decreasing degradation rate (k_D) of ENaCs (Table 1).

Relocation number (N_R) of an individual ENaC to the apical membrane

We also estimated how many times (N_R) individual ENaCs stay to the apical membrane state (Apical) after the first endocytosis process (Fig. 1). Thus, equation (15) based on $R_R = (k_R/(k_R + k_D))$ (see equation (14)) indicates the recycling number (R_N) how many times ENaCs are recycled to the apical membrane state (Apical) during the whole life of ENaCs after the first endocytosis process (Fig. 1).

$$N_R = \left(\frac{k_R}{k_R + k_D}\right) + \left(\frac{k_R}{k_R + k_D}\right)^2 + \left(\frac{k_R}{k_R + k_D}\right)^3 + \cdots\cdots = \sum_{i=1}^{\infty}\left(\frac{k_R}{k_R + k_D}\right)^i = \frac{k_R}{k_D} \qquad (15).$$

The calculating results are shown in Table 2. Application of PTKIs almost completely blocked the relocation to the apical membrane: PTKIs significantly diminished N_R ($= k_R/k_D$) by 95% from 0.400 ± 0.065 to 0.019 ± 0.002 (n = 6; p < 0.00025) due to a decrease in the value of $R_R = (k_R/(k_R + k_D))$ (Table 2).

Cumulative Na^+ absorption (I_{SC})

Another interesting point is how PTKs contribute to the cumulative Na^+ absorption (cumulative I_{SC} as coulombs). PTKIs treatment decreased the cumulative ENaC-mediated epithelial Na^+ transport by 35% from 185, 871 ± 7, 667 to 122, 238 ± 8, 399 μC/cm²/day (n = 6; p < 0.00025: Table 2). If the PTKIs-induced reduction in the cumulative Na^+ absorption (Table 2) would be caused only by the modulation of the intracellular ENaC trafficking, it depends on the time how long ENaCs stay in the apical membrane. Therefore, we estimated the residency time (T_{AM}) and the cumulative time (T_{CTAM}) of an individual ENaC staying in the apical membrane.

Table 2. Estimated values of the recycling ratio, R_R ($= (k_R/(k_R + k_D))$) (%) of ENaC and the relocation number how many times ENaC is relocated to the apical membrane state (Apical), N_R ($= k_R/k_D$) after the first retrieval, and the cumulative Na^+ absorption (I_{SC}) (μC/cm²/day) in the absence (control) and presence of PTKIs, AG1296 (10 μM) and AG1478 (10 μM). *, significantly different between control (n=6) and PTKIs (n=6) at p < 0.0001. #, significantly different between control (n=6) and PTKIs (n=6) at p < 0.00025

Condition	Recycling ratio, R_R ($=k_R/(k_R+k_D)$) (%)	Relocation number of ENaC to the apical membrane state, N_R ($=k_R/k_D$)	Cumulative Na^+ absorption (I_{SC}) (μC/cm²/day)
Control	27.83 ± 3.14	0.400 ± 0.065	185,871 ± 7,667
PTKIs	1.83 ± 0.22 *	0.019 ± 0.002 #	122,238 ± 8,399 #

Residency time of an individual ENaC in the apical membrane after insertion; T_{AM} (= $1/k_E$)

The reciprocal of the endocytotic rate of ENaC is its mean residency time in the apical membrane; T_{AM} (= $1/k_E$). The values of T_{AM} (= $1/k_E$) observed in the absence (control) and presence of PTKIs were respectively 4.010 ± 0.137 h (n = 6) and 4.035 ± 0.484 h (n = 6; no significant difference) (Table 3). This means that PTKs sensitive to AG1296 (10 μM) and AG1478 (10 μM) have no contribution to the residency time of an individual ENaC in the apical membrane after its insertion to the apical membrane.

Table 3. Residency time of ENaC in the apical membrane T_{AM}; how long an individual ENaC stays at the apical membrane each time after the insertion of ENaCs into the apical membrane ($T_{AM} = 1/k_E$) and the cumulative time how long an individual ENaC stays at the apical membrane during its whole life-time period before degradation ($T_{CTAM} = (1 + N_R)/k_E = (1+k_R/k_D)/k_E$), and whole life-time ($T_{WLT}$) after the first insertion to the apical membrane ($T_{WLT} = 1/k_E + N_R(1/k_R + 1/k_I + 1/k_E) + 1/k_D = 1/k_E + (k_R/k_D)\ (1/k_R + 1/k_I + 1/k_E) + 1/k_D$) in the absence (control) and presence of PTKIs, AG1296 (10 μM) and AG1478 (10 μM). *, significantly different between control (n=6) and PTKIs (n=6) at $p < 0.05$. #, significantly different between control (n=6) and PTKIs (n=6) at $p < 0.005$. NS, no significant difference between control (n=6) and PTKIs (n=6)

Condition	T_{AM} (= $1/k_E$)(h)	T_{CTAM} (h)	T_{WLT} (h)
Control	4.010 ± 0.137	5.603 ± 0.297	9.349 ± 1.004
PTKIs	4.035 ± 0.484 NS	4.110 ± 0.493 *	4.912 ± 0.431 #

Cumulative time of an individual ENaC residing in the apical membrane before degradation; T_{CTAM}

Although the mean residency time of an individual ENaC in the apical membrane is not regulated by PTKs sensitive to AG1296 (10 μM) and AG1478 (10 μM), we know that some parts of ENaCs are recycled to the apical membrane subsequently to the retrieval (see Table 2). Therefore, it is interesting to calculate the mean cumulative time (T_{CTAM}) that a channel will spend in the apical membrane before entering the degradative pathway, which reflects the cumulative Na^+ absorption. The T_{CTAM} is expressed as follows.

$$T_{CTAM} = (1 + N_R)\frac{1}{k_E} = \left(1 + \frac{k_R}{k_D}\right)\frac{1}{k_E} \qquad (16),$$

where N_R (see equation (15)) is the number how many times an individual ENaC is recycled to the apical membrane after the first retrieval. PTKIs treatment significantly decreased the value of T_{CTAM} by 27%: T_{CTAM}, 4.101 ± 0.493 h in PTKIs-treated cells (n = 6); 5.603 ± 0.297 h in control cells (n = 6; $p < 0.05$: Table 3). This decrease in T_{CTAM} caused by PTKIs treatment would be one of the reasons that the cumulative Na^+ absorption was reduced by PTKIs treatment. Indeed, PTKI treatment reduced the cumulative Na^+ absorption by 34% (Table 2). The PTKIs treatment-induced decrease in the cumulative Na^+ absorption would be a little bit larger than that in T_{CTAM} (27% in Table 2). This means that in addition to the PTKI-induced decrease in T_{CTAM}, the PTKI treatment would diminish the cumulative Na^+ absorption by affecting another factor contributing to the ENaC-mediated epithelial Na^+ transport, such as the open probability (activity) of ENaCs. However, even though some parts of PTKIs treatment-induced decrease in the cumulative Na^+ absorption might be caused by a decrease in the open probability of ENaC, the main cause of the PTKIs treatment-induced decrease in the cumulative Na^+ absorption would be the decrease in T_{CTAM} of ENaC.

Whole life-time of ENaC after the initial insertion to the apical membrane; T_{WLT}

We further studied the effect of PTKIs treatment on the whole life-time of ENaC (T_{WLT}) after the initial insertion of ENaC into the apical membrane. The whole life-time of ENaC (T_{WLT}) is determined by the following equation.

$$T_{WLT} = \frac{1}{k_E} + N_R\left(\frac{1}{k_R} + \frac{1}{k_I} + \frac{1}{k_E}\right) + \frac{1}{k_D} \qquad (17),$$

where N_R (equation (15)) is the number how many times an individual ENaC is recycled to the apical membrane after its first endocytosis from the apical membrane (the apical state: Apical) into the cytosolic space (the recycling state: Recycl). The values of T_{WLT} of ENaC after the first insertion into the apical membrane were respectively 9.349 ± 1.004 h in the absence of PTKIs (control) (n = 6) and 4.912 ± 0.431 h in the presence of PTKIs (n = 6; $p < 0.005$: Table 3), indicating that the treatment of the cells with PTKIs significantly shortened the T_{WLT}. This estimation suggests that PTKs sensitive to the PTKIs contribute to keep T_{WLT} longer.

Discussion

The present study indicates that PTKs contribute to the regulation of the intracellular ENaC trafficking: the rates of insertion, recycling and degradation. Our previous study [26] has reported that a hypotonic stress activates JNK/SAPK via receptor tyrosine kinases (RTKs) without any ligand application, 2) the RTK-JNK/SAPK cascade mediates the stimulatory action of the hypotonic stress on the ENaC-mediated epithelial Na^+ transport, and 3) PI3-kinase is involved in the RTK-JNK/SAPK cascade for the hypotonic stress-induced stimulation of the Na^+ transport. This study [26] has indicated that the treatment with PTKIs, AG1296 (10 μM) and AG1478 (10 μM), reduces the ENaC-mediated epithelial Na^+ transport. However, we have no information on how these PTKIs reduce the ENaC-mediated epithelial Na^+ transport. PI3-kinase regulates the intracellular trafficking and the activity (open probability) of ENaCs [36]: 1) PI3-kinase activates and recruits serum- and glucocorticoid-induced kinase 1 (SGK1) to ENaCs, regulating the endocytosis of ENaCs by phosphorylating (inactivating) Nedd4-2, and resulting in a longer stay of ENaCs in the apical membrane [37-39]; 2) PI3-kinase increases the activity (open probability) of ENaC by disinhibiting the ENaC-inhibitory pathway, Raf, via activation of SGK1 [40, 41].

The application of hypotonicity activates PI3-kinase via PTKs-mediated pathways [26], and the activity (open probability) of ENaC is maintained at a high level via the hypotonicity-induced activation of PI3-kinase [40, 41]. Therefore, PTKIs would inhibit the hypotonicity-activated PI3-kinase, decreasing the activity (open probability) of ENaC. In the present study, we indicate that the PTKIs-caused diminution of the hypotonicity-induced cumulative ENaC-mediated epithelial Na^+ transport (35%: Table 2) was a little bit larger than that estimated from the PTKI-caused diminution of the T_{CTAM} of ENaC under the hypotonic condition (27%: Table 3). The larger PTKIs-caused diminution of the hypotonicity-induced cumulative ENaC-mediated epithelial Na^+ transport than that of T_{CTAM} of ENaC would be partially due to a decrease in the activity (open probability) of ENaC caused by PTKIs, although PTKIs would diminish the hypotonicity-induced cumulative ENaC-mediated epithelial Na^+ transport mainly by decreasing T_{CTAM} of ENaC via a decrease in the recycling rate (k_R) and an increase in the degradation rate (k_D) (Table 1).

The mean value of whole life-time period of ENaC staying at the apical membrane before degradation, T_{CTAM}, was 5.60 h, meaning the half-life time of ENaC staying at the apical membrane is 3.88 h on an assumption that the number of ENaC proteins staying at the apical membrane with the life-time time period exponentially decreases against the time according the Boltzmann distribution. Gonzalez-Montelongo et al. [42] and Yu et al. [43] have reported the half-life time of ENaC staying at the apical membrane is 3 ~ 3.5 h. Therefore, the result on the mean value of whole life-time period of ENaC staying at the apical membrane before degradation, T_{CTAM}, is closed to that reported by Gonzalez-Montelongo et al. [42] and Yu et al. [43].

Our previous report [26] indicates that hypotonicity affects the ENaC trafficking via activation of PDGFR and EGFR without any ligands binding to the receptors by changing the membrane tension. Many investigators have studied the role of EGF and EGFR in the ENaC regulation [44, 45], however the contradictory results have been reported [44, 45]. Taruno et al. [26] have report that an inhibitor of EGFR diminishes the ENaC-mediated Na^+ transport in renal A6 epithelial cells by activating EGFR via the change in the membrane tension caused by hypotonicity, suggesting that activation of EGFR would have a stimulatory action on the ENaC-mediated Na^+ transport in renal A6 epithelial cells. Similar results [46, 47] have been reported that EGF activates the ENaC-mediated Na^+ transport via a PI3-kinase-mediated pathway, which is involved in the ENaC intracellular trafficking [48]. On the other hand, the application of EGF inhibits ENaCs: EGF diminishes the activity (open probability) of ENaC via an ErbB-receptor-mediated pathway [44, 49, 50]. At present, we could not clearly indicate the reason why the contradictory results have been reported regarding the effect of EGF on ENaC activity and the ENaC-mediated Na^+ transport. Activation of EGFR would activate variable signaling pathways after its activation such as PI3-kinase-, Rac1- and MAPK-dependent pathways by coupling ErbB2 receptor [44], which have the stimulatory or inhibitory action on the ENaC-mediated Na^+ transport. Further, the EGFR stimulation connects with hepatocyte growth factor [51]. The substrate of hepatocyte growth factor-regulated tyrosine substance (Hrs) is involved in the endosomal membrane trafficking [52], and Hrs binds ENaC controlling the intracellular ENaC trafficking [53]. Thus, in various types of cells EGF would show its stimulatory or inhibitory action on the ENaC-mediated Na^+ transport dependent on which type of signaling, the stimulatory or inhibitory pathway, connecting to EGFR, which couples with ErbB2 receptor in some cases [44]. These facts would cause the contradictory phenomena upon the application of EGF and PTKIs.

Conclusion

The present study indicates that application of EGFR and PDGFR-inhibitable PTKIs reduced the insertion rate (k_I), and the recycling rate (k_R) of ENaCs, but increased degradation rate (k_D) in renal A6 epithelial cells under a hypotonic condition. These observations indicate that hypotonicity increases the surface expression of ENaCs by increasing the insertion rate (k_I) and the recycling rate (k_R) of ENaCs associated with a decrease in the degradation rate but without any significant effects on the endocytotic rate (k_E) in EGFR and PDGFR-related PTKs-mediated pathways.

Acknowledgements

This work was supported by Grants-in-Aid from Japan Society of the Promotion of Science (JSPS KAKENHI Grant Number JP26713008 and JP16K15181 to AT, and JP15K15034 and 18H03182 to YM), Salt Science (1429 and 1542 to AT, and 1235 to YM), KIT-KPUM-KPU-KPhU Collaborative Research Grant (2013 and 2015) to YM, Society for Research on Umami Taste, Nestlé Nutrition Council, Japan to AT, Kyoto Prefectural Public University Corporation to AT, Kyoto-Funding for Innovation in Health-related R&D Fields to YM, Fuji Foundation for Protein Research to YM, and Cell Research Conference to YM.

Disclosure Statement

The authors declare that the research was conducted in the absence of any commercial or financial relationships that could be construed as a potential conflict of interest.

References

1 Aoi W, Niisato N, Sawabe Y, Miyazaki H, Marunaka Y: Aldosterone-induced abnormal regulation of ENaC and SGK1 in Dahl salt-sensitive rat. Biochem Biophys Res Commun 2006;341:376-381.
2 Aoi W, Niisato N, Sawabe Y, Miyazaki H, Tokuda S, Nishio K, Yoshikawa T, Marunaka Y: Abnormal expression of ENaC and SGK1 mRNA induced by dietary sodium in Dahl salt-sensitively hypertensive rats. Cell Biol Int 2007;31:1288-1291.
3 Marunaka Y: Characteristics and pharmacological regulation of epithelial Na^+ channel (ENaC) and epithelial Na^+ transport. J Pharmacol Sci 2014;126:21-36.
4 Marunaka Y: Importance of expression and function of angiotensin II receptor type 1 in pulmonary epithelial cells. Respir Physiol Neurobiol 2014;196:39-42.
5 Meneton P, Loffing J, Warnock DG: Sodium and potassium handling by the aldosterone-sensitive distal nephron: the pivotal role of the distal and connecting tubule. Am J Physiol Renal Physiol 2004;287:F593-601.
6 Mironova E, Bugaj V, Roos KP, Kohan DE, Stockand JD: Aldosterone-independent regulation of the epithelial Na^+ channel (ENaC) by vasopressin in adrenalectomized mice. Proc Natl Acad Sci U S A 2012;109:10095-10100.
7 Mironova E, Chen Y, Pao AC, Roos KP, Kohan DE, Bugaj V, Stockand JD: Activation of ENaC by AVP contributes to the urinary concentrating mechanism and dilution of plasma. Am J Physiol Renal Physiol 2015;308:F237-243.
8 Stockand JD: The role of the epithelial Na^+ channel (ENaC) in high AVP but low aldosterone states. Front Physiol 2012;3:304.
9 Vallon V, Lang F: New insights into the role of serum- and glucocorticoid-inducible kinase SGK1 in the regulation of renal function and blood pressure. Curr Opin Nephrol Hypertens 2005;14:59-66.
10 Verrey F, Loffing J, Zecevic M, Heitzmann D, Staub O: SGK1: aldosterone-induced relay of Na^+ transport regulation in distal kidney nephron cells. Cell Physiol Biochem 2003;13:21-28.
11 Salker MS, Steel JH, Hosseinzadeh Z, Nautiyal J, Webster Z, Singh Y, Brucker S, Lang F, Brosens JJ: Activation of SGK1 in endometrial epithelial cells in response to PI3K/AKT inhibition impairs embryo implantation. Cell Physiol Biochem 2016;39:2077-2087.
12 Salker MS, Hosseinzadeh Z, Alowayed N, Zeng N, Umbach AT, Webster Z, Singh Y, Brosens JJ, Lang F: LEFTYA Activates the Epithelial Na^+ Channel (ENaC) in Endometrial Cells via Serum and Glucocorticoid Inducible Kinase SGK1. Cell Physiol Biochem 2016;39:1295-1306.
13 Ding Y, Zhao R, Zhao X, Matthay MA, Nie HG, Ji HL: ENaCs as Both Effectors and Regulators of MiRNAs in Lung Epithelial Development and Regeneration. Cell Physiol Biochem 2017;44:1120-1132.
14 Butterworth MB, Edinger RS, Johnson JP, Frizzell RA: Acute ENaC stimulation by cAMP in a kidney cell line is mediated by exocytic insertion from a recycling channel pool. J Gen Physiol 2005;125:81-101.
15 Jans D, Simaels J, Cucu D, Zeiske W, Van Driessche W: Effects of extracellular Mg^{2+} on transepithelial capacitance and Na^+ transport in A6 cells under different osmotic conditions. Pflugers Arch 2000;439:504-512.
16 Marunaka Y, Eaton DC: Effects of vasopressin and cAMP on single amiloride-blockable Na channels. Am J Physiol Cell Physiol 1991;260:C1071-1084.
17 Marunaka Y, Hagiwara N, Tohda H: Insulin activates single amiloride-blockable Na channels in a distal nephron cell line (A6). Am J Physiol Renal Physiol 1992;263:F392-400.
18 Niisato N, Van Driessche W, Liu M, Marunaka Y: Involvement of protein tyrosine kinase in osmoregulation of Na^+ transport and membrane capacitance in renal A6 cells. J Membr Biol 2000;175:63-77.
19 Shimkets RA, Warnock DG, Bositis CM, Nelson-Williams C, Hansson JH, Schambelan M, Gill JR, Jr., Ulick S, Milora RV, Findling JW, Canessa CM, Rossier BC, Lifton RP: Liddle's syndrome: heritable human hypertension caused by mutations in the beta subunit of the epithelial sodium channel. Cell 1994;79:407-414.
20 Snyder PM, Price MP, McDonald FJ, Adams CM, Volk KA, Zeiher BG, Stokes JB, Welsh MJ: Mechanism by which Liddle's syndrome mutations increase activity of a human epithelial Na^+ channel. Cell 1995;83:969-978.

21 Firsov D, Schild L, Gautschi I, Merillat AM, Schneeberger E, Rossier BC: Cell surface expression of the epithelial Na channel and a mutant causing Liddle syndrome: a quantitative approach. Proc Natl Acad Sci U S A 1996;93:15370-15375.
22 Kamynina E, Debonneville C, Hirt RP, Staub O: Liddle's syndrome: a novel mouse Nedd4 isoform regulates the activity of the epithelial Na^+ channel. Kidney Int 2001;60:466-471.
23 Taruno A, Marunaka Y: Analysis of blocker-labeled channels reveals the dependence of recycling rates of ENaC on the total amount of recycled channels. Cell Physiol Biochem 2010;26:925-934.
24 Sasamoto K, Marunaka R, Niisato N, Sun H, Taruno A, Pezzotti G, Yamamoto T, Kanamura N, Zhu W, Nishio K, Inui T, Eaton DC, Marunaka Y: Analysis of aprotinin, a protease inhibitor, action on the trafficking of epithelial Na^+ channels (ENaC) in renal epithelial cells using a mathematical model. Cell Physiol Biochem 2017;41:1865-1880.
25 Sasamoto K, Niisato N, Marunaka Y: Aprotinin reduces the recycling rate of epithelial Na^+ channels (ENaC) to the apical membrane of an epithelial cell: a four-state model of intracellular ENaC trafficking. J Physiol Sci 2017;67:S84.
26 Taruno A, Niisato N, Marunaka Y: Hypotonicity stimulates renal epithelial sodium transport by activating JNK via receptor tyrosine kinases. Am J Physiol Renal Physiol 2007;293:F128-138.
27 Sun H, Niisato N, Inui T, Marunaka Y: Insulin is involved in transcriptional regulation of NKCC and the CFTR Cl^- channel through PI3K activation and ERK inactivation in renal epithelial cells. J Physiol Sci 2014;64:433-443.
28 Sasamoto K, Niisato N, Marunaka Y: Simulation of Cl^- secretion in epithelial tissues: New methodology estimating activity of electroneutral Cl^- transporter. J Physiol Sci 2016;66:S89.
29 Sun H, Niisato N, Nishio K, Hamilton KL, Marunaka Y: Distinct action of flavonoids, myricetin and quercetin, on epithelial Cl^- secretion: useful tools as regulators of Cl^- secretion. BioMed Res Int 2014;2014:902735.
30 Kleyman TR, Cragoe Jr. EJ: Cation transport probes: the amiloride series. Methods Enzymol 1990;191:739-755.
31 Niisato N, Eaton DC, Marunaka Y: Involvement of cytosolic Cl^- in osmoregulation of alpha-ENaC gene expression. Am J Physiol Renal Physiol 2004;287:F932-939.
32 Kleyman TR, Yulo T, Ashbaugh C, Landry D, Cragoe E Jr, Karlin A, Al-Awqati Q: Photoaffinity labeling of the epithelial sodium channel. J Biol Chem 1986;261:2839-2843.
33 Niisato N, Driessche WV, Liu M, Marunaka Y: Involvement of protein tyrosine kinase in osmoregulation of Na^+ transport and membrane capacitance in renal A6 cells. J Membr Biol 2000;175:63-77.
34 Niisato N, Marunaka Y: Activation of the Na^+-K^+ pump by hyposmolality through tyrosine kinase-dependent Cl^- conductance in Xenopus renal epithelial A6 cells. J Physiol 1999;518:417-432.
35 Taruno A, Niisato N, Marunaka Y: Intracellular calcium plays a role as the second messenger of hypotonic stress in gene regulation of SGK1 and ENaC in renal epithelial A6 cells. Am J Physiol Renal Physiol 2008;294:F177-186.
36 Soundararajan R, Lu M, Pearce D: Organization of the ENaC-regulatory machinery. Crit Rev Biochem Mol Biol 2012;47:349-359.
37 Debonneville C, Flores SY, Kamynina E, Plant PJ, Tauxe C, Thomas MA, Munster C, Chraibi A, Pratt JH, Horisberger JD, Pearce D, Loffing J, Staub O: Phosphorylation of Nedd4-2 by Sgk1 regulates epithelial Na^+ channel cell surface expression. EMBO J 2001;20:7052-7059.
38 Flores SY, Loffing-Cueni D, Kamynina E, Daidie D, Gerbex C, Chabanel S, Dudler J, Loffing J, Staub O: Aldosterone-induced serum and glucocorticoid-induced kinase 1 expression is accompanied by Nedd4-2 phosphorylation and increased Na^+ transport in cortical collecting duct cells. J Am Soc Nephrol 2005;16:2279-2287.
39 Snyder PM, Olson DR, Thomas BC: Serum and glucocorticoid-regulated kinase modulates Nedd4-2-mediated inhibition of the epithelial Na^+ channel. J Biol Chem 2002;277:5-8.
40 Soundararajan R, Melters D, Shih IC, Wang J, Pearce D: Epithelial sodium channel regulated by differential composition of a signaling complex. Proc Natl Acad Sci USA 2009;106:7804-7809.
41 Thomas SV, Kathpalia PP, Rajagopal M, Charlton C, Zhang J, Eaton DC, Helms MN, Pao AC: Epithelial sodium channel regulation by cell surface-associated serum- and glucocorticoid-regulated kinase 1. J Biol Chem 2011;286:32074-32085.
42 Gonzalez-Montelongo R, Barros F, Alvarez de la Rosa D, Giraldez T: Plasma membrane insertion of epithelial sodium channels occurs with dual kinetics. Pflugers Arch 2016;468:859-870.

43 Yu L, Helms MN, Yue Q, Eaton DC: Single-channel analysis of functional epithelial sodium channel (ENaC) stability at the apical membrane of A6 distal kidney cells. Am J Physiol Renal Physiol 2008;295:F1519-1527.
44 Zheleznova NN, Wilson PD, Staruschenko A: Epidermal growth factor-mediated proliferation and sodium transport in normal and PKD epithelial cells. Biochim Biophys Acta 2011;1812:1301-1313.
45 Staruschenko A, Palygin O, Ilatovskaya DV, Pavlov TS: Epidermal growth factors in the kidney and relationship to hypertension. Am J Physiol Renal Physiol 2013;305:F12-20.
46 Markadieu N, Crutzen R, Blero D, Erneux C, Beauwens R: Hydrogen peroxide and epidermal growth factor activate phosphatidylinositol 3-kinase and increase sodium transport in A6 cell monolayers. Am J Physiol Renal Physiol 2005;288:F1201-1212.
47 Levchenko V, Zheleznova NN, Pavlov TS, Vandewalle A, Wilson PD, Staruschenko A: EGF and its related growth factors mediate sodium transport in mpkCCDc14 cells via ErbB2 (neu/HER-2) receptor. J Cell Physiol 2010;223:252-259.
48 Pearce D: SGK1 regulation of epithelial sodium transport. Cell Physiol Biochem 2003;13:13-20.
49 Tong Q, Stockand JD: Receptor tyrosine kinases mediate epithelial Na^+ channel inhibition by epidermal growth factor. Am J Physiol Renal Physiol 2005;288:F150-161.
50 Pavlov TS, Levchenko V, O'Connor PM, Ilatovskaya DV, Palygin O, Mori T, Mattson DL, Sorokin A, Lombard JH, Cowley AW Jr, Staruschenko A: Deficiency of renal cortical EGF increases ENaC activity and contributes to salt-sensitive hypertension. J Am Soc Nephrol 2013;24:1053-1062.
51 Carpenter BL, Chen M, Knifley T, Davis KA, Harrison SM, Stewart RL, O'Connor KL: Integrin alpha6beta4 Promotes Autocrine Epidermal Growth Factor Receptor (EGFR) Signaling to Stimulate Migration and Invasion toward Hepatocyte Growth Factor (HGF). J Biol Chem 2015;290:27228-27238.
52 Urbe S, Mills IG, Stenmark H, Kitamura N, Clague MJ: Endosomal localization and receptor dynamics determine tyrosine phosphorylation of hepatocyte growth factor-regulated tyrosine kinase substrate. Mol Cell Biol 2000;20:7685-7692.
53 Zhou R, Kabra R, Olson DR, Piper RC, Snyder PM: Hrs controls sorting of the epithelial Na^+ channel between endosomal degradation and recycling pathways. J Biol Chem 2010;285:30523-30530.